3-12-2023

A Simulation Study of Surfactant/Foam Processes in Shallow Subsurface Remediation: Using Foams for Mobility Control vs. Blockage

Betty Cepeda
Louisiana State University and Agricultural and Mechanical College

A SIMULATION STUDY OF SURFACTANT/FOAM PROCESSES IN SHALLOW SUBSURFACE REMEDIATION: USING FOAMS FOR MOBILITY-CONTROL VS. BLOCKAGE

A Thesis

Submitted to the Graduate Faculty of the
Louisiana State University and
Agricultural and Mechanical College
in partial fulfillment of the
requirements for the degree of
Master of Petroleum Engineering

in

The Craft and Hawkins Department of Petroleum Engineering

by
Betty Cepeda
B.S., Escuela Superior Politecnica del Litoral, 2018
May 2023

To my family in Ecuador, maybe they did notice my calls were for something else other than asking for mom's recipe. To my husband, let's move through life as capybaras and seahorses. Finally, to the world of people I've met in Louisiana, y'all made it *more better*.

Acknowledgments

This work was made possible by the data and aid provided by Rural Research Institute (the research branch of Korea Rural Community Corporation) of the Republic of Korea, and by the generous donation from Computer Modeling Group of their simulator products CMG STARS and CMG CMOST. We also extend our gratitude to the Fulbright Commission both in the US and Ecuador for contributing to the realization of this work.

Table of Contents

Illustrations

Tables

Figures

Abstract

Many shallow ex-situ and in-situ remediation treatments come from the contamination of underground soils and groundwater sources by organic hydrocarbon components called non-aqueous phase liquids (NAPLs). These contaminants, if leaking, can impose long-term threats causing environmental and health concerns. One of the versatile in-situ remediation techniques is using surfactant/foam processes that can overcome subsurface heterogeneity and improve NAPL removal.

This simulation study investigates surfactant/foam processes, especially focusing on two different roles of foams during the treatment: foams for "mobility control" vs. foams for "blocking". The first is based on the actual operations carried out in the pilot-test site for 23 days (i.e., 20 days of surfactant followed by 3 days of foam injection, in a line-drive pattern with 3 injection wells and 3 extraction wells), while the second is to evaluate the potential of blocking foams by placing foams downstream (i.e., foam injected into the downstream extraction wells, but surfactant is still injected into the upstream injection wells).

The results show that (i) the use of mobility-control foams together with surfactant injection can improve and accelerate oil removal from the site (about 91.9 % oil recovery in this particular case investigated), and (ii) based on 24 scenarios, the use of blocking foams is as efficient as, or more efficient than, mobility-control foams, exhibiting the oil recovery up to near 94.9 %. This outcome of this study is believed to help design an improved way of applying surfactant/foam processes.

Chapter 1. Introduction

Many shallow subsurface remediation issues stem from the contamination of underground soils and associated groundwater sources by organic hydrocarbon components, commonly called non-aqueous phase liquids (NAPLs). After leaching into underlying aquifers, these contaminants can impose long-term threats causing environmental and health concerns, if untreated (Wang and Mulligan, 2004).

Remediation options include treatments in its original location (in-situ) or elsewhere where the contaminated aquifer material is taken out to be processed and returned to the original location (ex-situ). Examples of ex-situ remediation techniques include anaerobic bioremediation, soil washing, and low-temperature thermal desorption (Bianco et al., 2020; Gerhard et al., 2020) to name a few. Some common in-situ techniques consist of extracting polluted water (i.e., pump and treat) or injecting base fluids (typically water) with different types of additives (such as biological materials, chemical species, and nanoparticles) (Yuniati, 2018; Zhang et al., 2019; Prakash et al., 2021). Among these in-situ techniques, one particular type that has seen a steady increase during the past decade is surfactant enhanced aquifer remediation (SEAR). The increased use of surfactant chemicals is because of their ability to create one or more beneficial conditions such as altering the wettability of the media through adsorption, reducing the level of capillary trapping of NAPLs by lowering interfacial tension, and dissolving contaminants to form emulsified droplets (Zhong et al., 2003; Wang and Mulligan, 2004; Um et al., 2013; Liu et al., 2021).

When applying surfactant and foam process to a particular site, the SEAR treatment can be followed by foam injection, which is typically carried out by injecting gas and surfactant together (co-injection) or injecting gas into the media with pre-existing surfactant molecules.

Foam in porous media as a dispersion of internal gas phase trapped by the surrounding external surfactant-laden liquid phase, forming liquid foam films (called lamellae), can block the gas flow and thus control the gas-phase mobility (Rossen, 1996). Some previous field studies demonstrate that foams can help sweep the geological layers with permeability contrast and thus improve NAPL removal (Szafranski et al., 1998; Mulligan and Eftekhari, 2003), which is based on the characteristics of foam stability in porous media (i.e., more stable foams in the high permeability layers due to the low capillary pressure environment, eventually resulting in a reduced flow capacity) (Rossen, 1996). In other applications, foams are applied as a delivering agent (i.e., capturing and transporting solid particles with increased interfacial area between gas and liquid) or as a diverting agent (i.e., foams occupying the high permeability area, changing the course of the subsequent fluids (with chemical reactants)), trying to reach out to the area or layer of interest (Shen et al., 2011; Roostapour et al., 2014). These improved benefits from using foams in remediation treatments are possible due to the foam's ability to overcome subsurface heterogeneity, control the mobility of gas phases, and mitigate gravity segregation (Kovscek and Radke, 1994; Rossen, 1996; Rossen and van Duijin, 2004; Lee and Kam, 2013). There are examples in the literature on how one can model foam propagation in shallow in-situ remediations (Mayberry et al., 2008; Lee et al., 2014) and in deep vadose zone remediation managed by Hanford nuclear reservation site (Roostapour and Kam, 2012). These efforts typically accommodate the presence of foam in the media by using a factor called "mobility reduction factor" (MRF) in the transport equation: for example, MRF = 1 being no foams (i.e., typical gas-water flow), $1 < MRF < 50$ foams with relatively low flow resistance (i.e., weak foams), and $MRF > 50$ foams with relatively high flow resistance (strong foams). Using foams in these applications has its own challenges as well. For example, foam stability might be too

sensitive to certain types of organic compounds (Karthick et al., 2019), or it might be too difficult in some cases to predict the rheological properties of foams because of complicated in-situ dynamics of foam creation and coalescence mechanisms (Gauglitz et al., 2002; Namdar-Zanganeh et al., 2011).

Apart from those benefits mentioned above, foams exhibit another type of versatility, that is, functioning as a blocking agent. Common examples are associated with using foams for shutting off gas or water influx in near-wellbore applications (Hanssen and Dalland, 1990; Cheng et al., 2000; Turta and Singhal, 2002) or for stopping high-permeability streaks near the wells (Blaker et al., 2002; Portois et al., 2018). These concepts are originated from earlier attempts to use foams for gas leak sealant for petroleum reservoirs, successfully reducing the gas leak virtually to zero (Bernard and Holm, 1970). While the term "blocking" might give the impression of an absolute obstruction to gas flow, it oftentimes refers to a very low value of effective gas permeability, near the range of 1 to 2 x 10^{-13} m^2 (or 0.1 - 0.2 darcy range, equivalently) (Hanssen and Dalland, 1994).

Chapter 2. Motivation and Objectives

This study is motivated by previous in-situ assessment and remediation studies of multiple spill sites on a military base, South Korea. The contaminants identified in the field include both light and dense NAPLs (i.e., benzene, toluene, ethylbenzene, and xylene, trichloroethene (TCE), and tetrachloroethene (PCE)) that leaked from storage tanks, transportation pipelines, and distributions facilities. The early stage of the investigation focused on the field-scale assessment through underground soil and water sampling, creation of resistivity logs, water injectivity/extraction tests for SEAR treatment, and screening tests for various types of surfactants and contaminants (Um et al., 2013). The next stage focused on the site-scale pilot test to examine how the injected fluids such as surfactant and foam would propagate under the level of existing subsurface heterogeneity and help remove contaminants from the site. Some examples of these scenarios are shown in Fleifel et al. (2020) and Cepeda-Salgado et al. (2022), for instance, how computer simulations can be applied to match oil production history helping subsurface characterization, and how different scenarios of alternating surfactant and foam injection can impact the overall oil recovery from the treatment.

This simulation study is performed to investigate the application of surfactant/foam processes, especially focusing on the two different roles of foams during the treatment: foams for "mobility control" vs. foams for "blocking". More specifically, the first task is to history match oil recovery from the actual pilot test (i.e., 20 days of surfactant followed by 3 days of mobility-control foam injection, in a line-drive pattern with 3 injection wells and 3 extraction wells). This task is believed to demonstrate how mobility-control foams can improve oil recovery by taking advantage of prior surfactant injection.

The second task is to evaluate the potential of blocking foams by placing foams

downstream (i.e., foam injected into the downstream extraction wells (rather than injection wells), while surfactant is still injected into the upstream injection wells). In order to keep consistency, the same 23 days of treatment is tested (i.e., 20 days of surfactant followed by 3 days of foam and surfactant injection; each of the last 3 days repeated with “blocking-foam injection downstream” in the morning followed by “surfactant injection upstream” for the rest of the day).

Chapter 3. Methodology

3.1. Governing and transport equations

This study uses Computer Modelling Group (CMG) software, STARS, which is designed for simulating multiphase flow in porous media with multiple phases and chemical species (CMG, 2020). The governing partial differential equation for material balance, as shown below, can be applied to various in-situ remediation treatments:

$$\frac{\partial}{\partial t}\left(\phi \sum_{j=1}^{N_p} \rho_j S_j \omega_{ij} + (1-\phi)\rho_s \omega_{is}\right) + \nabla\left(\sum_{j}^{N_p} \rho_j \omega_{ij} \vec{u}_j - \phi S_j \vec{k}_{ij} \nabla \omega_{ij}\right) = \phi \sum_{j=1}^{N_p} S_j r_{ij} + (1-\phi) r_{is} \quad \ldots\ldots(1)$$

where ϕ represents the porosity, ω_{ij} mass fraction, ρ_j and ρ_s density, S_j saturation, $\vec{u}_j$ velocity vector, $\vec{k}_{ij}$ dispersion coefficient tensor, and r_{ij} and r_{is} chemical reactions. Note that subscripts i, j, and s represent components, fluid phases, and solid phase respectively.

The convection term can be related to the pressure field through Darcy's transport equation for each phase. For example, the flow of phase j can be expressed as follows in one-dimensional space:

$$\frac{Q_j}{A} = u_j = \frac{K k_{rj}}{\mu_j} \frac{\Delta P_j}{L} \quad \ldots\ldots (2)$$

where Q_j, u_j, and μ_j are the flow rate, velocity, and viscosity of phase j respectively; $\frac{\Delta P_j}{L}$ the pressure gradient through phase j; A and K the cross-sectional area and absolute permeability of the medium; and k_{rj} the relative permeability to phase j. Depending on flow direction, the permeability terms can be further clarified as K_h (i.e., horizontal permeability) or K_v (i.e., vertical

permeability). This study deals with three different phases (j = w (water), o (oil), and g (gas)), and the surfactant chemicals as a constituent dissolved in the water phase.

Transport of gas phase in the presence of foam can be expressed by modifying the equation for the gas phase, i.e., when subscript j = g (gas),

$$\frac{Q_g}{A} = u_g = \frac{Kk_{rg}}{\mu_g MRF}\frac{\Delta P_g}{L} \qquad \text{……..(3)}$$

where the mobility reduction factor (MRF) of the gas phase accounts for additional pressure drop exerted by foam liquid films (if liquid films are present, MRF > 1; otherwise MRF = 1 (no foam)).

The term, total flow rate (Q_j), can be defined by using water flow rate (Q_w) and gas flow rate (Q_g), i.e.,

$$Q_t = Q_g + Q_w \qquad \text{……. (4)}$$

and also by using water flowing fraction (f_w) and gas flowing fraction (f_g) i.e.,

$$Q_t = f_g Q_t + f_w Q_t = f_g Q_t + (1 - f_g) Q_t \qquad \text{……. (5)}$$

where f_g is also commonly referred to as foam quality during foam process (Kovscek and Radke, 1994), and $f_w + f_g = 1$ from material balance.

3.2. Description of investigation site

The military base of interest, as shown in Fig. 1(a), houses a number of fuel storage tanks and distribution pipelines. The underlying aquifer contains both light and dense NAPL contaminants,

as confirmed by examining soil and groundwater samples taken at different locations and by performing resistivity log tests within the base (Um et al., 2013). Among six vertical cross-sectional contour maps in Fig. 1(b), this study focuses on the cross-section denoted by number "3" (where the concrete foundation with a building structure is located). The pilot test site is located at the upper right-hand-side corner of Fig. 1(c). Note that the red-colored area in Fig. 1(c) represents the region with higher resistivity values measured, meaning higher concentration of NAPLs. While the military base is reported to have both light and dense NAPL spills, this specific site for the pilot-scale in-situ remediation test shows light NAPLs only.

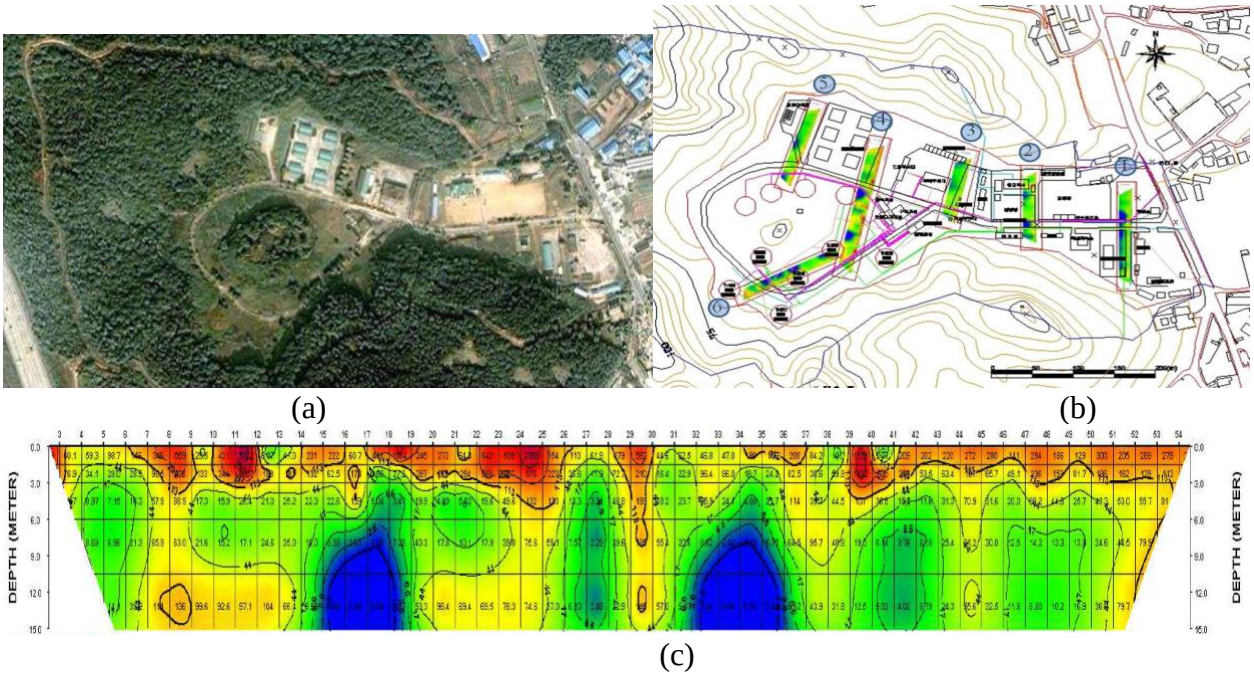

Figure 1. Military base of interest: (a) photo of the field; (b) site map with contour lines and resistivity-log cross-sections ("1" through "6"); and (c) resistivity-log cross-section ("3" in (b)) containing the pilot-test site *Source: Courtesy of Korean Rural Community Corporation*

The pilot test site is formed by 3 injection wells and 3 extraction wells (5m x 5 m coverage) with 3 m depth, as shown by Figs. 2(a) and 2(b). The wells are named as North, Middle, South injection wells (Inj-N, Inj-M, Inj-S) and North, Middle, South extractions wells (Ext-N, Ext-M, Ext-S). There is one monitoring well in between only for fluid sampling purpose,

and thus does not play a role in fluid injection or production during the remediation treatment. A combination of finer grids (the major treatment area) and coarser grids (the surrounding area) are used in computer simulations, as shown in Fig. 2(c), resulting in 42 x 42 x 10 blocks representing 10.5 m x 10.5 m x 3 m, and 39 x 39 x 10 blocks representing 19.5 m x 19.5 m x 3 m, respectively. Field sampling tests show that the groundwater table is about 0.30 m (above which gas saturation (S_g) is about 5.0 %). Oil saturation (S_o) for the treatment area (Fig. 2(b)), which can be as high as 16 % locally, has the average value of 5.0 %. This oil saturation corresponds to the initial oil volume of 0.327 m^3 within the treatment area.

Fig. 2(c) shows the level of heterogeneity associated with this site. This study follows the approach employed by Cepeda-Salgado et al. (2022) where the absolute permeability distribution captures the areal heterogeneity, while the net-to-gross (NTG) ratio captures the vertical heterogeneity (Note that the NTG term, which is between 0 and 1, represents the volume fraction of porous media available to flow, accounting for (or excluding) the volume occupied by non-contributing constituents such as clay minerals). The details are as follows: three horizontal permeability (K_h) values such as K_{ha} = 9.5, K_{hb} = 1.6, and K_{hc} = 0.26 darcies (note that 1 darcy is equivalent to 10^{-12} m^2 approximately), and three NTG values for the vertical layers such as NTG = 0.581 for layer 1 ($0 < z < 0.3$ m), NTG = 0.302 for layer 2 to 4 ($0.3 < z < 1.2$ m), and NTG = 0.289 for layer 5 to 10 ($1.2 < z < 3.0$ m).

(a)

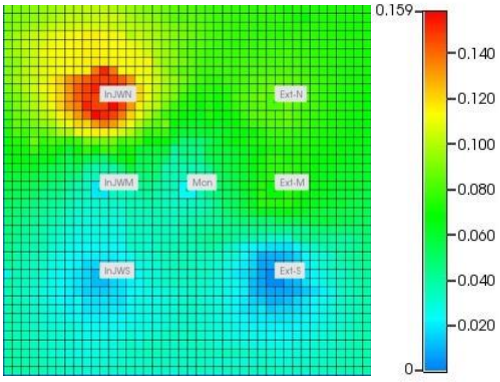

(b)

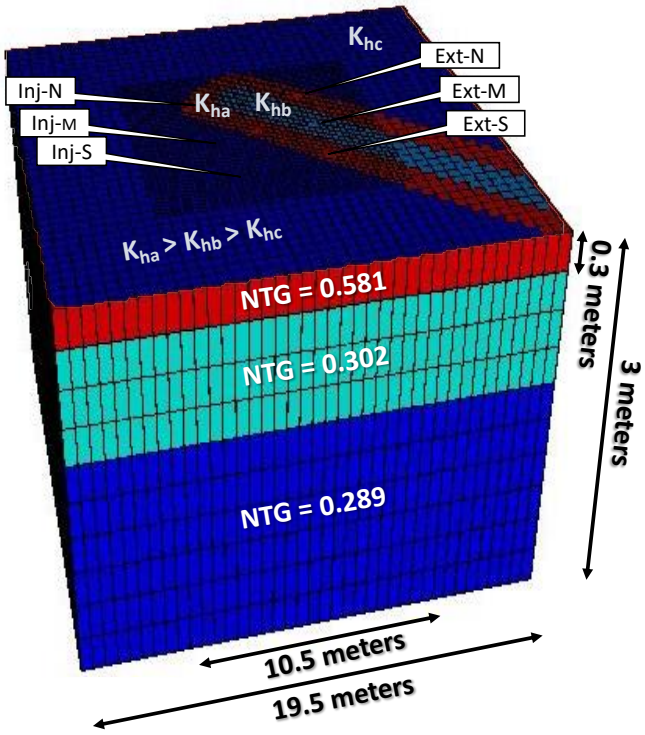

(c)

Figure 2. In-situ remediation site of interest: (a) photo of the actual pilot test site; (b) initial oil saturation distribution; and (c) areal and vertical heterogeneity in the site *Source: Figure 2(a) Courtesy of Korean Rural Community Corporation*

These three NTG values are originated from the fact that layer 1 is an interval right underneath the concrete pavement, layer 2-4 is an interval with added foreign soils and compactions to make a solid foundation for the fuel distribution facilities, and layer 5-10 is an interval with the original well-compacted soils. The vertical permeability (K_v) value is estimated to be a tenth of the horizontal permeability (K_v) value at any given locations.

Chapter 4. Results and discussions

In order to perform numerical simulations for this site, the following physical properties are employed as a part of input data: the connate water saturation (S_{wc}) = 0.2, residual oil saturation (S_{or}) = 0.0, residual gas saturation (S_{gr}) = 0.0, porosity (ϕ) = 8.75 %, water density (ρ_w) = 1.04 g/cc, oil density (ρ_o) = 0.68 g/cc, water viscosity (μ_w) =1.0 cp, and oil viscosity (μ_o) = 0.70 cp. All wells (both injection and extraction) are perforated uniformly along the entire vertical direction, unless otherwise noted.

4.1. Matching the production history of 12-days surfactant and mobility-control foam injection

The in-situ remediation treatment was designed with three operation phases (Phase 1, Phase 2, and Phase 3) consisting of a total of 23 operation days: Phase 1 is the first 10 days of surfactant injection with numerous samples collected at the extraction wells, Phase 2 is the second 10 days of surfactant injection with produced fluid samples taken only at the end of the period, and Phase 3 as the last 3 days of mobility-control foam injection (or, continuous injection of air and surfactant solution). Because of the limited accessibility to the site within the military base, each day is made up of 9 hours of active working time (8 am to 5 pm) followed by 15 hours of shut-in time (5 pm to 8 am). The total injection rate (Q_t) applied in the site is kept at Q_t = 2.30 m^3/day (or Q_t = 0.0958 m^3/hr, equivalently) for each injection well (i.e., $Q_t = Q_w$ = 2.30 m^3/day during Phases 1 and 2 (20 days surfactant only injection), and $Q_t = Q_g + Q_w$ = 1.848 m^3/day + 0.462 m^3/day = 2.30 m^3/day (meaning $f_g = Q_g/Q_t$ = 0.80) during Phase 3 (3 days foam injection)).

Fig. 3(a) shows the cumulative oil production history from all three extraction wells – x marks show part of data points from collected samples, while square marks show the trend of average values (for Day 1, 2, 3 and 10) with a sketch of the upper and lower ends to guide simulation studies. (Some x marks below the lower-end curve are neglected in the analysis

because they are taken before or after the operation each day. Fig. 3(b) shows simulation results at various MRF values (MRF = 1, 10, 100, and 500) to examine the effect of foam strength. The case of MRF = 100 is of interest in particular, as the MRF value is observed from column tests (Um et al., 2013). Overall, the case of MRF = 500 predicts the production history near the upper end, while the cases of MRF = 1 and 10 predict near the lower end. The case of MRF = 100 sits between the upper and lower ends, showing the amounts of total oil recovered at the end of Phase 3 to be 0.3008 m^3 (corresponding to 91.9 % oil recovery).

This simulation result fits the reported oil recovery from the pilot test (about 90 to 91%) reasonably well. Comparing this outcome with the amounts of cumulative oil recovered at the end of Phase 2, this is, 0.2944 m^3 (corresponding to 90.0 % oil recovery), one can see how much the last 3 days of foam injection for mobility-control purpose helped accelerate oil production overcoming the heterogeneity. Although not shown here, another simulation effort was tried to reveal that more than 20 days of additional surfactant injection after Phase 2 (without foams) would be required to produce this amount of remaining oil with a long tail. For comparison, Fig. 3(b) shows the simulations at MRF = 1 (i.e., gas -water co-injection with no foams), 10, and 500 leading to 0.2804, 0.2836, and 0.3037 m^3 oil recovery (or 85.7, 86.7, and 92.9 % recovery), respectively.

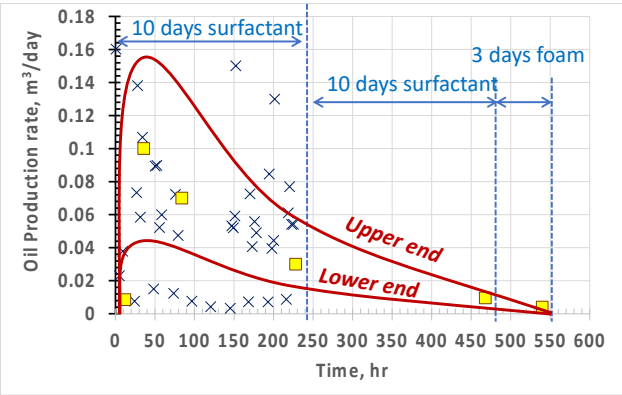

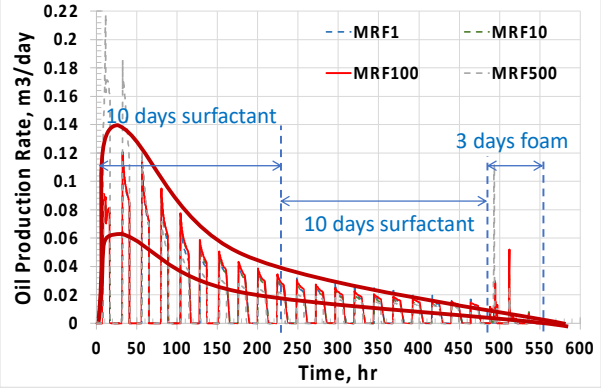

(a) (b)

Figure 3. Surfactant/foam remediation treatment for 23 days: (a) total oil production rate from all three extraction wells with upper and lower ends (x marks from individual sample test data and square marks from daily averages); and (b) simulation fit to the trend with different values of foam strength (MRF = 1, 10, 100, and 500)

Fig. 4 presents more details about the history matching with MRF = 100 shown in Fig. 3(b) - oil production rate as well as cumulative oil recovery from each of three wells (Ext-N, Ext-M, and Ext-S) in Fig. 4(a), and oil saturation distributions at different depths (layer, 1, 3, and 7) at the end of each of three operation phases (Phase 1, 2, and 3) in Fig. 4(b). The saturation distributions at the end of Day 10 and Day 20 show that whenever the NAPL contaminants, originally trapped by high level of clay contents, have an opportunity to travel laterally, they also migrate upwards (due to low oil density) and are produced from the top layer. The saturation distributions at the end of Day 23 show that the injected foams sweep the media more efficiently overcoming subsurface heterogeneity.

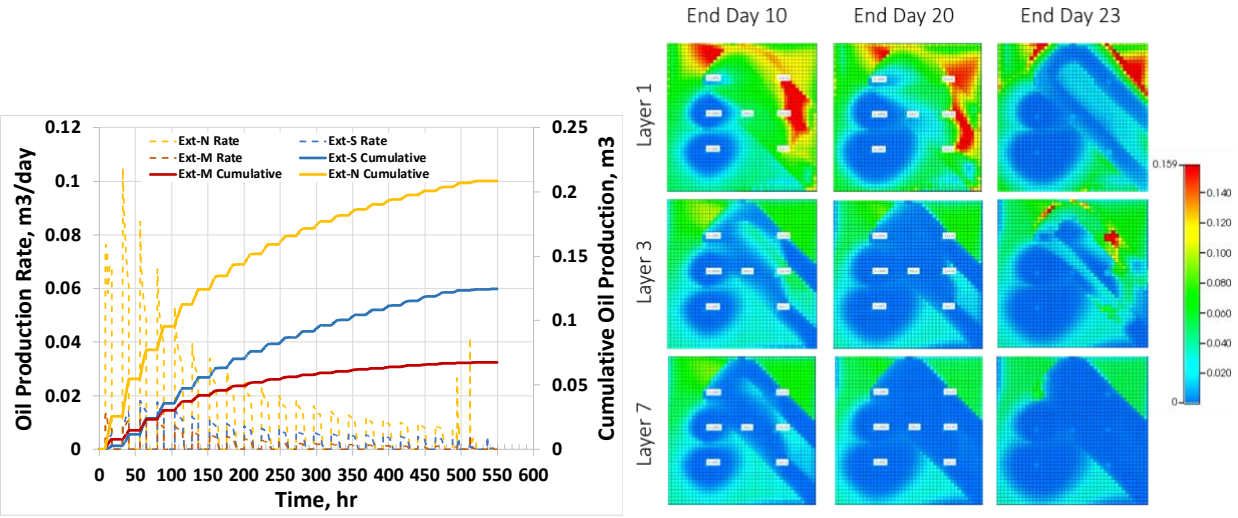

(a) (b)

Figure 4. Simulation results for the remediation treatment at MRF = 100: (a) individual-well oil production history (rate and cumulative recovery); and (b) snapshot of oil saturation at the end of each of three treatment phases (Phase 1 and 2 with surfactant injection; Phase 3 with foam injection)

4.2. Evaluation of using foams for blocking purposes

The next step is to evaluate the feasibility of using foams for blocking purpose. To keep consistency, the simulation efforts repeat the same Phase 1 and Phase 2 (i.e., first 20 days), but only consider changes in Phase 3 (i.e., last 3 days). More specifically, during those 3 days in Phase 3, foams are first injected into certain extraction wells for a pre-specified injection time (Δt_{foam}; 0.5, 1.0, 1.5, and 2 hours) early in the morning, and then the surfactant solution is injected from the three injection wells (Inj-N, Inj-M, and Inj-S) keeping foam-injected extraction wells downstream shut-in for the rest of the day. In all cases, the same injection rate (Q_t) is applied (i.e., Q_w = 2.30 m^3/day (surfactant injection in Phase 1 and 2); Q_g = 1.848 m^3/day, Q_w = 0.462 m^3/day, and MRF = 100 (foam injection in Phase 3); and Q_w = 2.30 m^3/day (surfactant injection in Phase 3)).

4.2.1. Injectivity test for foams introduced into extraction wells

As a starting point, it is necessary to examine how foams injected into the extraction wells (Ext-N, Ext-M, and Ext-S) would propagate into the system. In the simulations this study, it can be achieved by implementing hypothetical secondary foam injection wells (for example, Inj-BN, Inj-BM, Inj-BS) where the existing extraction wells are located.

Fig. 5 shows the response of foam injectivity test at Δt_{foam} = 0.5, 1.0, 1.5, and 2 hours in terms of gas saturation in the top layer (or, the top view of layer 1; Fig. 5(a)) and along the vertical cross-sectional area (or, the side view of the plane containing all extraction wells; Fig. 5(b)), when foams are injected at the beginning of Day 21 following Phase 1 and 2. The result in Fig. 5(a) allows the range of Δt_{foam} applied in this study to be determined. For example, Δt_{foam} < 0.5 hr is believed to be too short to place a meaningful amount of foams in the media (together with difficulties associated with such a short operation time), while Δt_{foam} > 2.0 hr is too long and

potentially places too much foam in the media that might push NAPL contaminants out of the treatment area. In addition, the result in Fig. 5(b) shows how the injected foams block the region around the extraction wells. In is interesting to find that even though the perforations are made along the entire depth, the majority of foams enter the media only through the upper 4 layers (layer 1 through 4). This is due to the relatively low gas density as well as higher NTG values.

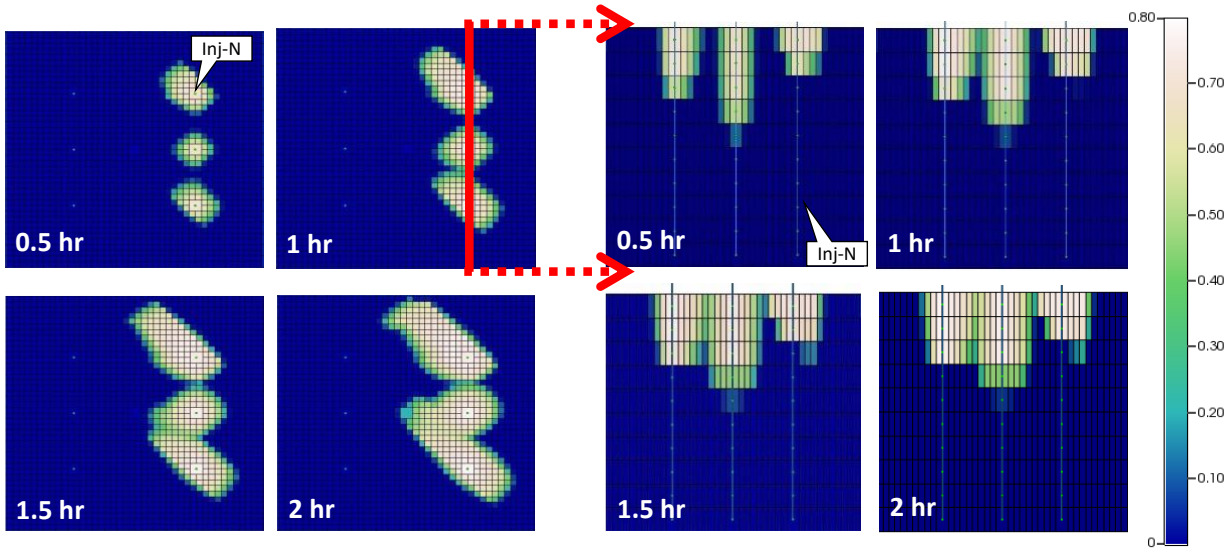

(a) (b)

Figure 5. Simulation of foam injectivity test (represented by gas saturation) from the extraction wells during foam injection time of 0.5, 1, 1.5 and 2.0 hours: (a) areal view of top layer (layer 1); and (b) side view of the plane containing 3 extraction wells

4.2.2. Results from various blocking scenarios

The next series of simulations evaluate two different situations, with each consisting of three possible cases, i.e., foams injected only into one of the wells (i.e., Ext-N, Ext-M, or Ext-S; so-called "single-well" blockage)) or foam injected into two of the wells (i.e., Ext-N and Ext-S, Ext-M and Ext-S, or Ext-N and Ext-M; so-called "dual-well" blockage). As explained above, the extractions wells selected for foam injection are kept shut-in during the subsequent surfactant

injection. For example, if foams are injected into Ext-N during Δt_{foam} hours, the remaining two wells (Ext-M and Ext-S) are open for oil recovery during the following (9 - Δt_{foam}) hours of surfactant injection into Inj-N, Inj-M, Inj-S wells. Because there are 4 different values of Δt_{foam} investigated (i.e., 0.5, 1.0, 1.5, and 2 hours), a total of 24 simulation scenarios are taken into consideration (i.e., 2 situations x 3 cases x 4 Δt_{foam} values).

Fig. 6 shows first six scenarios when Δt_{foam} = 0.5 hours in terms of oil production rate and cumulative oil recovery for single-well blockage (Fig. 6(a)) and dual-well blockage situations (Fig. 6(b)). Well name in the legend section represents which of the extraction wells are used for foam injection. In the case of cumulative oil recovery, the results are also compared with simulation results of the pilot test (i.e., 20 days of surfactant followed by 3 days of mobility-control foam injection; Figs. 2 and 3)). In all 6 scenarios in Fig. 6, using foams for blocking purpose is shown to be as efficient as, or more efficient than, the actual pilot-test simulation results.

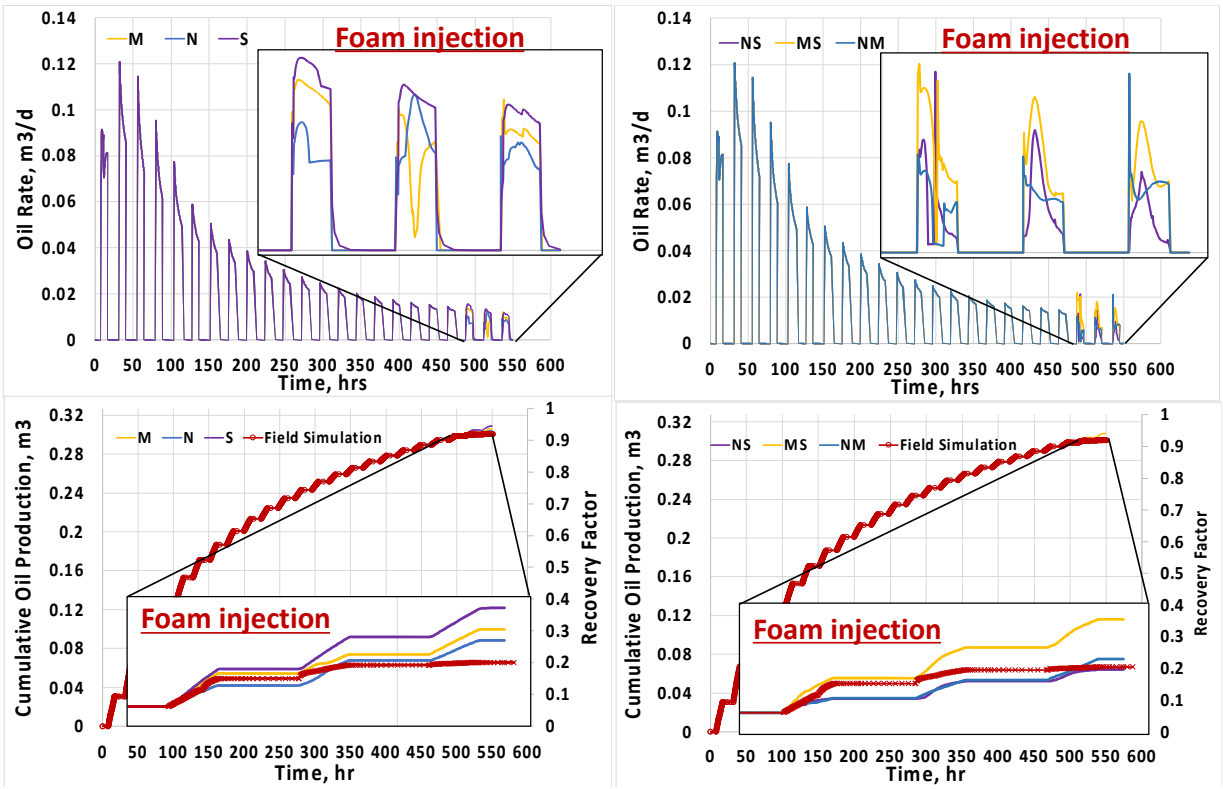

(a) (b)

Figure 6. Oil recovery from blocking foam application (0.5 hours of foam injection): (a) single-well blockage; and (b) dual-well blockage ("Field Simulation" curve shows oil recovery from mobility-control foam in Fig. 3 for comparison)

Figs. 7 through 9 show similar simulation results when Δt_{foam} = 1.0, 1.5, and 2.0 hours, respectively. It is interesting to find that, in all scenarios considered, the results are consistent with those in Fig. 6, demonstrating the effectiveness of using foams for blocking purpose. In fact, none of the 24 scenarios show any clear indications of inferior performance compared to the use of mobility-control foams. In particular, two best scenarios exhibiting the highest oil recovery are Ext-S single-well blockage with Δt_{foam} = 2 hours (94.84 % recovery) and Ext-M and Ext-S dual-well blockage with Δt_{foam} = 1 hour (94.92 % recovery).

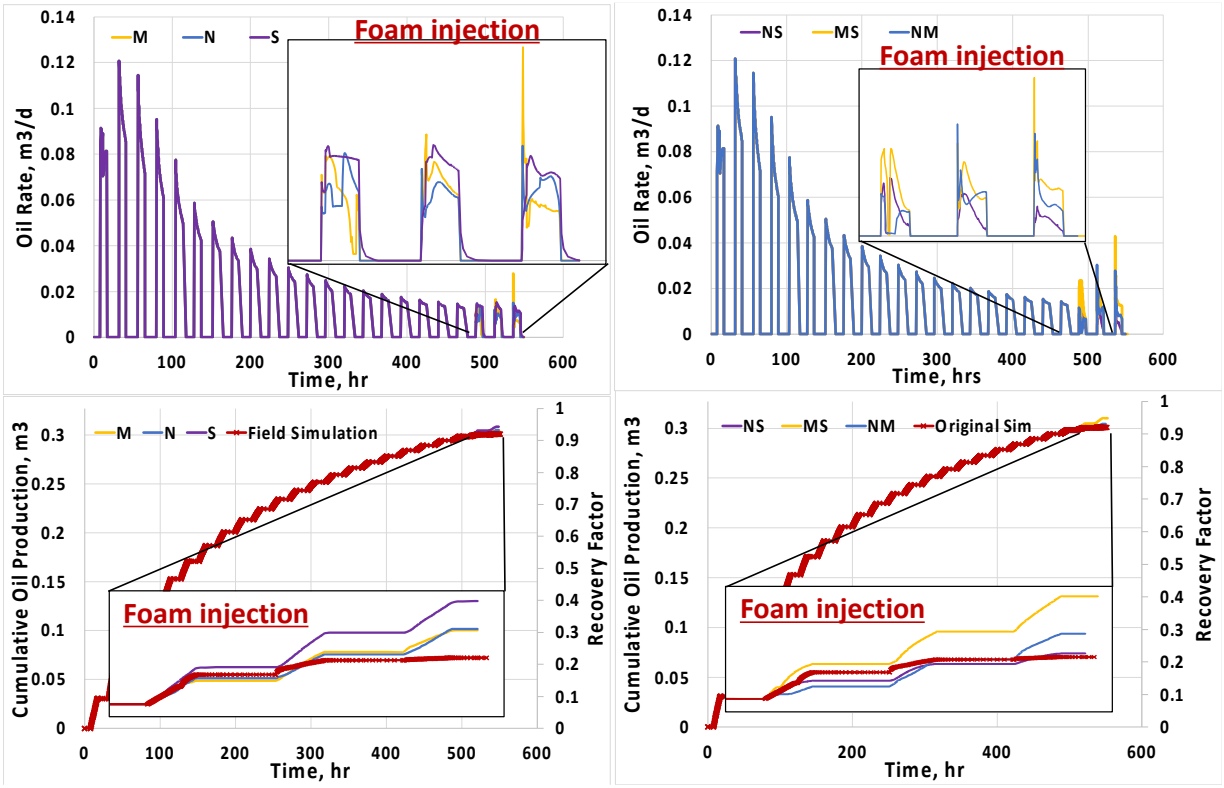

(a) (b)

Figure 7. Oil recovery from blocking foam application (1.0 hours of foam injection): (a) single-well blockage; and (b) dual-well blockage ("Field Simulation" curve shows oil recovery from mobility-control foam in Fig. 3 for comparison)

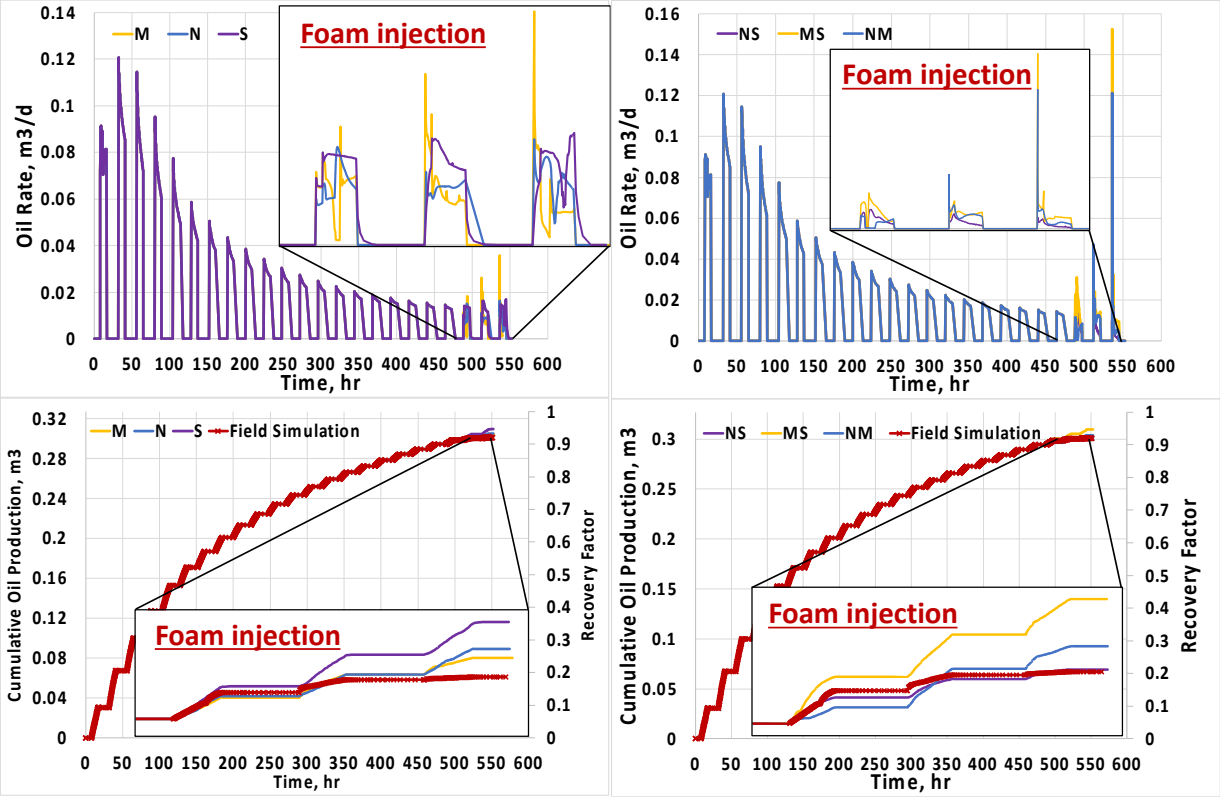

(a) (b)

Figure 8. Oil recovery from blocking foam application (1.5 hours of foam injection): (a) single-well blockage; and (b) dual-well blockage ("Field Simulation" curve shows oil recovery from mobility-control foam in Fig. 3 for comparison)

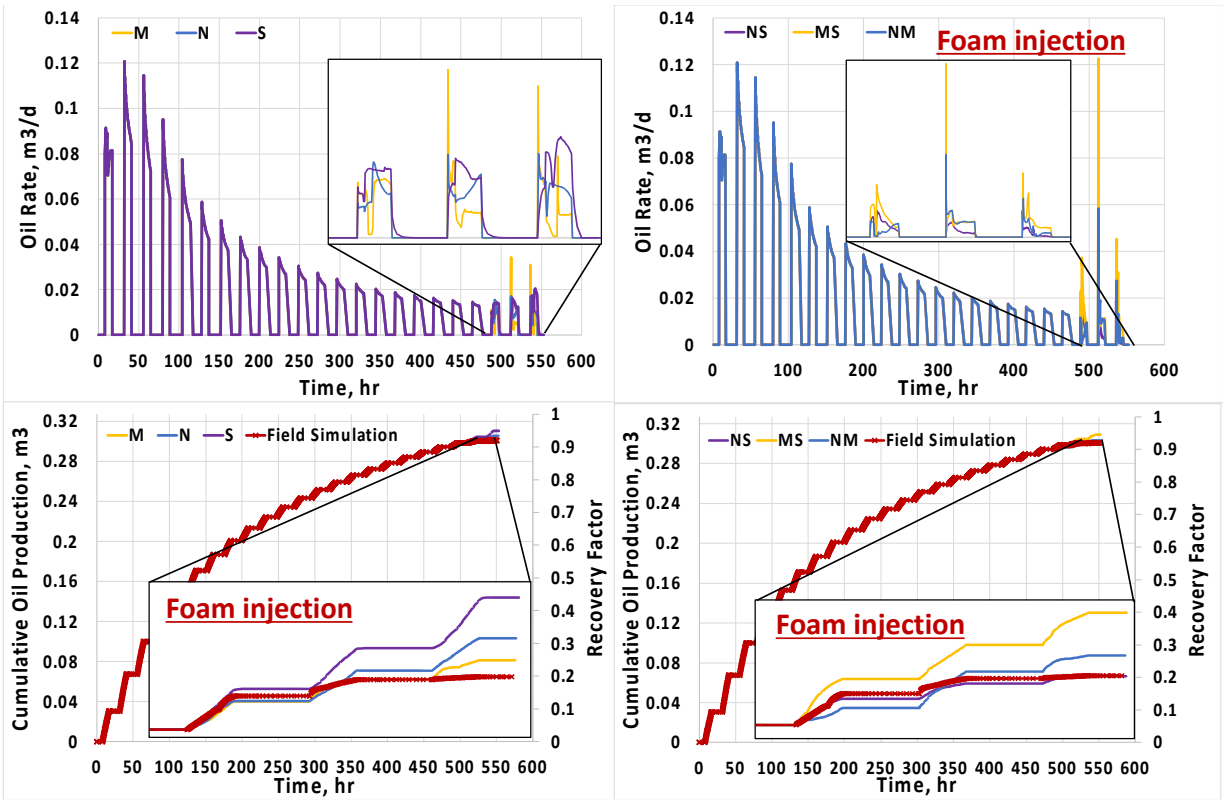

(a) (b)

Figure 9. Oil recovery from blocking foam application (2.0 hours of foam injection): (a) single-well blockage; and (b) dual-well blockage ("Field Simulation" curve shows oil recovery from mobility-control foam in Fig. 3 for comparison)

Fig. 10 shows oil saturation distribution for these two best scenarios. Compared to the mobility-control foams (i.e., Fig. 4, showing 91.9 % recovery), the improvement by using blocking foams is caused by two main aspects. First, the injected foams successfully block (as intended) the areas with low permeability (near Ext-M), areas far away from the main flow path between Inj-N and Ext-N (near Ext-S), and areas with low oil saturation (near Ext-M and Ext-S). Second, the foams injected for blocking purpose actually displace hard-to-reach oils out such that the subsequent surfactant injection can mobilize the oils more easily. Some of the unfavored behaviors observed by mobility-control foams – building too higher pressure gradient and thus displacing oils into the lower layers (layer 2 and layer 3) as shown in Fig. 4 – do not occur when

foams are used as a blocking agent. This tendency of containing the contaminants better within the treatment area, as observed, seems to be another benefit of using blocking foams.

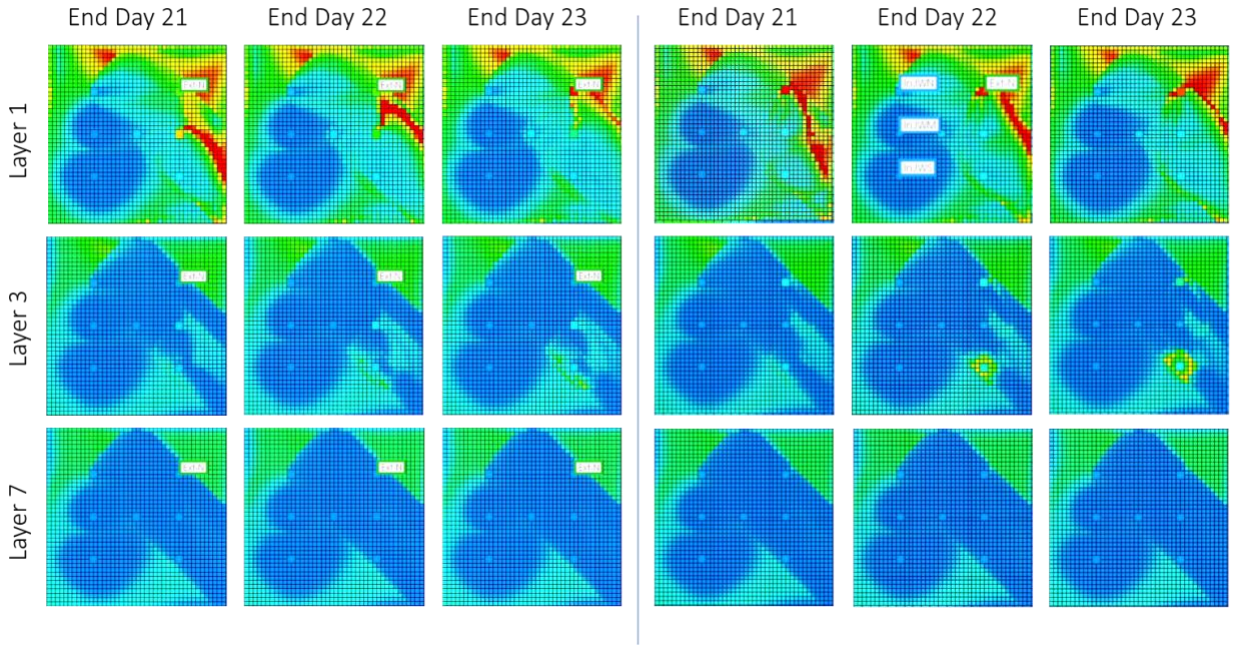

Figure 10. Oil saturation distribution during the last 3 days of foam treatment from the two best scenarios: (a) single-well blockage (Ext-S well; 2 hours foam injection); and (b) dual-well blockage (Ext-M and Ext-S wells; 1 hour foam injection)

Fig. 11 and Table 1 present the summary results of all 24 scenarios in terms of total cumulative recovery as well as recovery factor, in comparison with mobility-control foams.

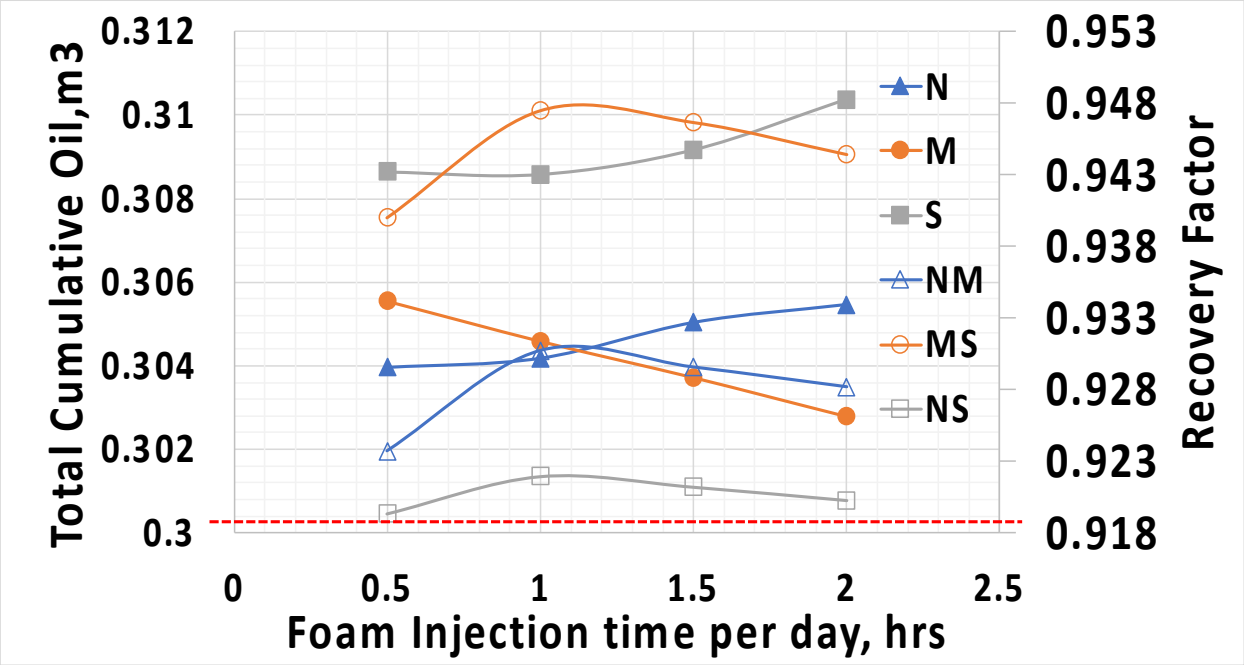

Figure 11. Summary of cumulative oil recovery and recovery factor from various blocking-foam injection scenarios compared with mobility-control foam injection (red-dashed line; 91.9 % recovery) (see Table 1 for more details)

Table 1. Summary of all blocking-foam injection scenarios

	0.5 Hours			1 Hours			1.5 Hours			2 Hours		
Well(s)	Total (m3)	RF	Change (%)	Total (m3)	RF	Change (%)	Total (m3)	RF	Change (%)	Total (m3)	RF	Change (%)
N	0.3040	0.930	1.05	0.3042	0.930	1.12	0.3050	0.933	1.40	0.3055	0.934	1.55
M	0.3056	0.934	1.57	0.3046	0.931	1.26	0.3037	0.929	0.97	0.3028	0.926	0.66
S	0.3086	0.944	2.60	0.3086	0.944	2.58	0.3092	0.945	2.78	0.3104	0.949	3.18
NS	0.3005	0.919	-0.12	0.3014	0.922	0.18	0.3011	0.921	0.09	0.3008	0.920	-0.01
MS	0.3076	0.941	2.24	0.3101	0.948	3.09	0.3098	0.947	3.00	0.3091	0.945	2.74
NM	0.3020	0.923	0.38	0.3044	0.931	1.18	0.3040	0.930	1.05	0.3035	0.928	0.89

Notes: ("% change" is from the comparison with mobility-control foam injection; RF represents recovery factor; and the highlighted shows two best scenarios from the simulations)

4.3. Effect of using lower-layer perforations for blocking foam injection

In line with the findings above associated with blocking foams, a question is raised to see

if injecting the blocking foams into the lower portion of the wells (where the NTG values are low) makes any differences.

Fig. 12 shows what happens when foams are injected in the same manner for the two best cases, but with the perforations only from layer 5 to layer 10 kept open. Figs. 12(a) ad 12(b) show areal distribution (layer 5) and vertical distribution of gas saturation with time. Even though the lower portion of the wells are specifically targeted for foam injection, foam tends to rise quickly and forms blocking walls similarly. This implies that the efforts to inject blocking foams into the lower portion of wells may not change the oil recovery significantly.

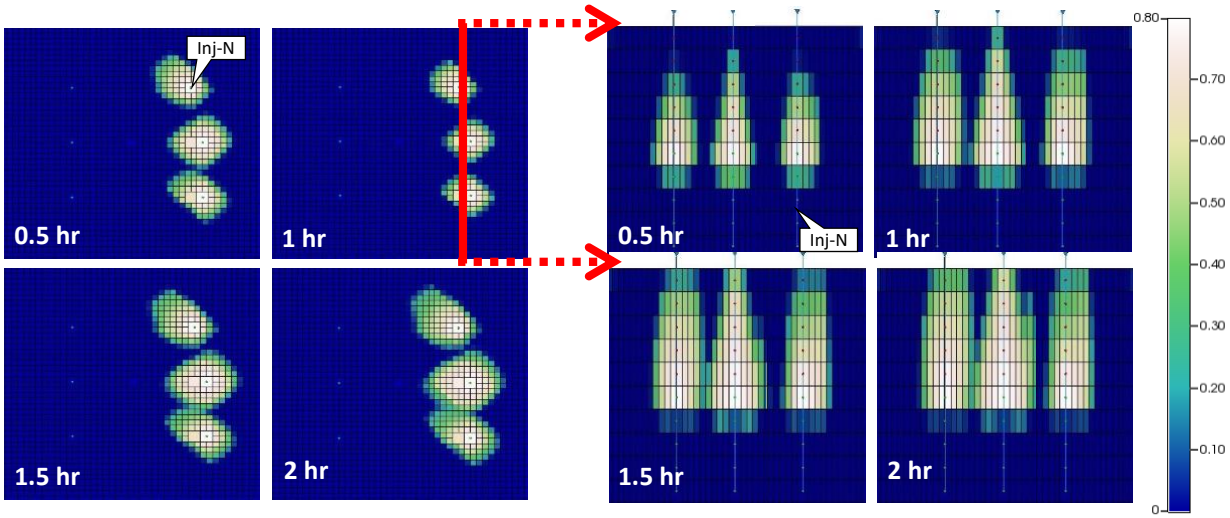

(a) (b)

Figure 12. Simulation of lower-layer foam injectivity test (represented by gas saturation) from the extraction wells during foam injection time of 0.5, 1, 1.5 and 2.0 hours: (a) aerial view of layer 5; and (b) side view of the plane containing 3 extraction wells

Figs. 13 and 14 show the results and they are consistent with this intuition. The two best scenarios now with only lower perforations (layer 5 through 10) exhibit the oil recovery of 94.27 % (cf. 94.84 % recovery for full perforations above) for Ext-S single-well blockage with Δt_{foam} = 2 hours, and the oil recovery of 94.71 % (cf. 94.92 % recovery for full perforations above) for Ext-M and Ext-S dual-well blockage with Δt_{foam} = 1 hour. These numbers are slightly lower compared to the cases with full perforations, but the differences are negligible.

It should be noted that this scenario of using partial lower-layer perforations for blocking foam injection is about light NAPLs, and therefore the impact on dense NAPL treatment might be different.

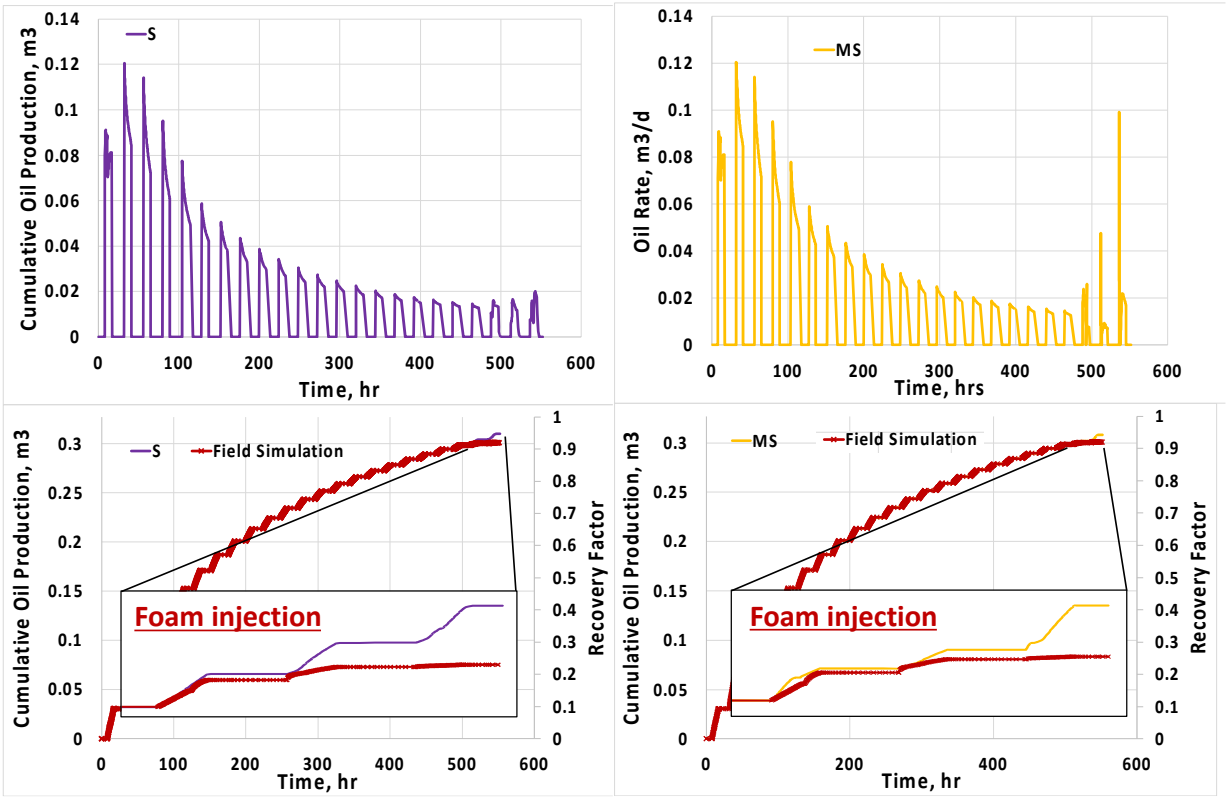

(a) (b)

Figure 13. Oil recovery when lower-layer foam injection is applied to the two best scenarios selected above: (a) single-well blockage (Ext-S well and 2 hours foam injection); and (b) dual-well blockage (Ext-M and Ext-S wells and 1 hour foam injection) ("Field Simulation" curve shows oil recovery from mobility-control foam in Fig. 3 for comparison)

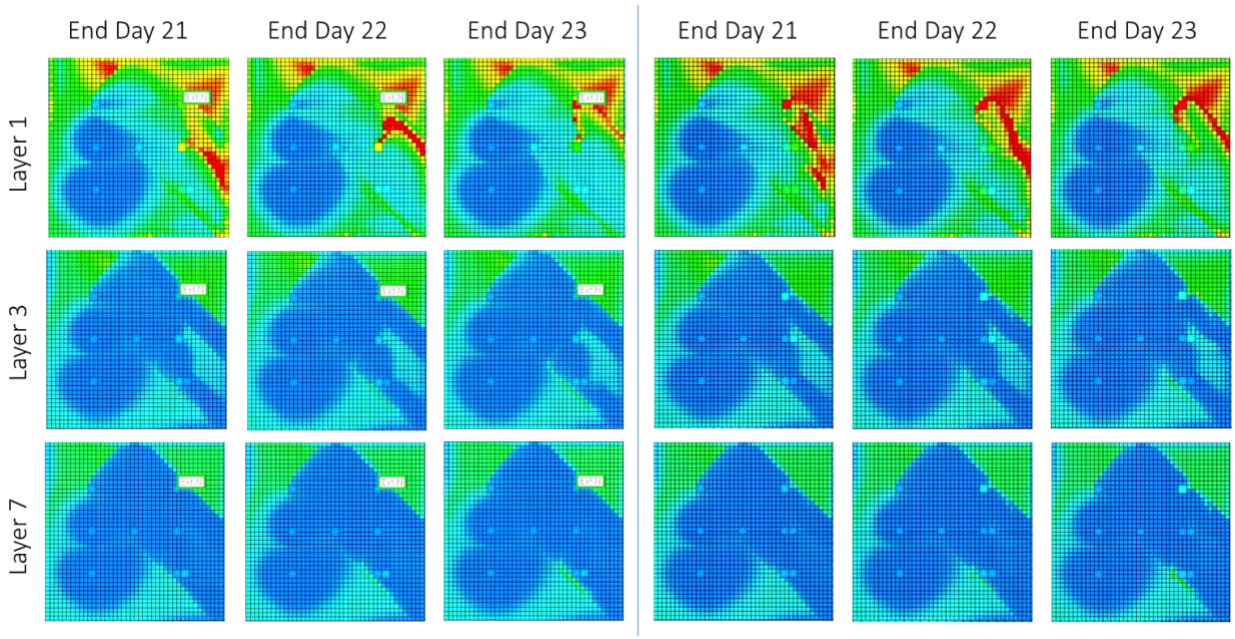

Figure 14. Oil saturation distribution during the last 3 days of lower-layer foam injection treatment applied to the two best scenarios selected above: (a) single-well blockage (Ext-S well and 2 hours foam injection); and (b) dual-well blockage (Ext-M and Ext-S wells and 1 hour foam injection) (cf. Fig. 10)

Chapter 5. Conclusions

For the in-situ remediation site of interest contaminated by light NAPLs (i.e., about 5 m x 5 m area with 3 m depth; average oil saturation of about 5 %), this study is carried out to (i) history-match the oil production during 23 days of surfactant (20 days) and foam (3 days for mobility-control purpose) treatment in a line drive pattern with 3 injection wells and 3 extraction wells, and (ii) evaluating the potential of using foams for blocking purpose downstream. The major findings of this simulation study can be summarized as follows:

- The pilot test and related computer simulations demonstrate that the use of mobility-control foams together with surfactant injection can improve and accelerate oil removal from the site (about 91.9 % oil recovery in this particular case investigated). The level of gas-phase mobility reduction during foam process (i.e., MRF) is an important design parameter that can come from separate surfactant-screening tests.
- When foams are evaluated for blocking purpose (i.e., foams introduced into the extraction wells downstream first, then followed by the subsequent surfactant injection into the original injection wells), most of the 24 scenarios (using different combinations of wells and foam injection durations downstream) show that using blocking foams is as efficient as, or more efficient than, mobility-control foams. In particular, the outcomes of two scenarios are shown to be standing out, exhibiting the oil recovery of 94.84 % (Ext-S single-well blockage with 2 hour foam injection) and 94.92 % (Ext-M and Ext-S dual-well blockage with 1 hour foam injection), compared to 91.9 % oil recovery from the case of mobility-control foams applied in the pilot test. It is because these blocking foams not only divert the subsequent surfactant solutions into the more desirable locations, but also displace hard-to-reach contaminants out of the disadvantaged locations near the

wells.

- The use of partial perforations for blocking foam injection (i.e., foam injection specifically targeted into the lower portion of wells) is also compared with the use of full perforations along the vertical direction. This particular well design does not show much difference between the two cases, because the injected foams occupy the vicinity of the extraction wells equally effectively. This finding is based on the light NAPL contaminants as shown in this study, and its applicability to dense NAPL contaminants is still unknown.

References

Bernard, G. G., & Holm, L. (1970). Model Study of Foam as a Sealant for Leaks in Gas Storage Reservoirs. Society of Petroleum Engineers Journal, 10(01), 9–16. https://doi.org/10.2118/2353-pa

Bianco, F., Monteverde, G., Race, M., Papirio, S., & Esposito, G. (2020). Comparing performances, costs and energy balance of ex situ remediation processes for PAH-contaminated marine sediments. Environmental Science and Pollution Research, 27(16), 19363–19374. https://doi.org/10.1007/s11356-020-08379-y

Blaker, T., Aarra, M. G., Skauge, A., Rasmussen, L., Celius, H. K., Martinsen, H. A., & Vassenden, F. (2002). Foam for Gas Mobility Control in the Snorre Field: The FAWAG Project. SPE Reservoir Evaluation &Amp; Engineering, 5(04), 317–323. https://doi.org/10.2118/78824-pa

Cepeda-Salgado, B., Fleifel, H., Lee, G. S., & Kam, S. I. (2022). A simulation study of in-situ NAPL remediation treatment by using surfactant and foam processes in a military base South Korea. Journal of Contaminant Hydrology, 247, 103982. https://doi.org/10.1016/j.jconhyd.2022.103982

Cheng, L., Reme, A., Shan, D., Coombe, D., & Rossen, W. (2000). Simulating Foam Processes at High and Low Foam Qualities. SPE/DOE improved oil recovery symposium. https://doi.org/10.2118/59287-ms

CMG (Computer Modeling Group Ltd), 2020. STARS, BUILDER User Guide.

Fleifel, H., Izadi, M., Park, S., Gupta, I., Lee, G., & Kam, S. I. (2020). Shallow Subsurface Environmental Remediation by Using Tracer–Surfactant–Foam Processes: History-Matching and Performance Prediction. Transport in Porous Media, 134(3), 565–592. https://doi.org/10.1007/s11242-020-01458-1

Gauglitz, P. A., Friedmann, F., Kam, S. I. & Rossen, W. (2002). Foam Generation in Homogeneous Porous Media. Chemical Engineering and Science, 57 (19): 4037–4052. https://doi.org/10.1016/S0009-2509(02)00340-8.

Gerhard, J. I., Grant, G. P., & Torero, J. L. (2020). Star: a uniquely sustainable in situ and ex situ remediation process. Sustainable Remediation of Contaminated Soil and Groundwater, 221–246. https://doi.org/10.1016/b978-0-12-817982-6.00009-4

Hanssen, J., & Dalland, M. (1990). Foams for Effective Gas Blockage in the Presence of Crude Oil. All Days. https://doi.org/10.2118/20193-ms

Hanssen, J. E., & Dalland, M. (1994). Gas-Blocking Foams. Advances in Chemistry, 319–353. https://doi.org/10.1021/ba-1994-0242.ch008

Karthick, A., Chauhan, M., Krzan, M., & Chattopadhyay, P. (2019). Potential of surfactant foam stabilized by Ethylene glycol and Allyl alcohol for the remediation of diesel contaminated soil. Environmental Technology &Amp; Innovation, 14, 100363. https://doi.org/10.1016/j.eti.2019.100363

Kovscek, A., & Radke, C. (1994). Fundamentals of foam transport in porous media. ACS Advances in Chemistry Series. https://doi.org/10.2172/10192736

Lee, S., & Kam, S. (2013). Enhanced Oil Recovery by Using CO2 Foams. Enhanced Oil Recovery Field Case Studies, 23–61. https://doi.org/10.1016/b978-0-12-386545-8.00002-6

Lee, S., Lee, G., & Kam, S. I. (2014). Three-Phase Fractional Flow Analysis for Foam-Assisted Non-aqueous Phase Liquid (NAPL) Remediation. Transport in Porous Media, 101(3), 373–400. https://doi.org/10.1007/s11242-013-0250-y

Liu, J. W., Wei, K. H., Xu, S. W., Cui, J., Ma, J., Xiao, X. L., Xi, B. D., & He, X. S. (2021). Surfactant-enhanced remediation of oil-contaminated soil and groundwater: A review. Science of the Total Environment, 756, 144142. https://doi.org/10.1016/j.scitotenv.2020.144142

Mayberry, D. J., Afsharpoor, A., & Kam, S. I. (2008). The Use of Fractional-Flow Theory for Foam Displacement in Presence of Oil. SPE Reservoir Evaluation &Amp; Engineering, 11(04), 707–718. https://doi.org/10.2118/100964-pa

Mulligan, C. N., & Eftekhari, F. (2003). Remediation with surfactant foam of PCP-contaminated soil. Engineering Geology, 70(3–4), 269–279. https://doi.org/10.1016/s0013-7952(03)00095-4

Portois, C., Boeije, C. S., Bertin, H. J., & Atteia, O. (2018). Foam for Environmental Remediation: Generation and Blocking Effect. Transport in Porous Media, 124(3), 787–801. https://doi.org/10.1007/s11242-018-1097-z

Prakash, A. A., Prabhu, N. S., Rajasekar, A., Parthipan, P., AlSalhi, M. S., Devanesan, S., & Govarthanan, M. (2021). Bio-electrokinetic remediation of crude oil contaminated soil enhanced by bacterial biosurfactant. Journal of Hazardous Materials, 405, 124061. https://doi.org/10.1016/j.jhazmat.2020.124061

Roostapour, A., & Kam, S. (2012). Modeling foam delivery mechanisms in deep vadose-zone remediation using method of characteristics. Journal of Hazardous Materials, 243, 37–51. https://doi.org/10.1016/j.jhazmat.2012.09.014

Roostapour, A., Lee, G., Zhong, L., & Kam, S. (2014). Model fit to experimental data for foam-assisted deep vadose zone remediation. Journal of Hazardous Materials, 264, 460–473. https://doi.org/10.1016/j.jhazmat.2013.09.016

Rossen, W. R. (1996). Foams in Enhanced Oil Recovery. Foams, 413–464. https://doi.org/10.1201/9780203755709-11

Rossen, W., & van Duijn, C. (2004). Gravity segregation in steady-state horizontal flow in homogeneous reservoirs. Journal of Petroleum Science and Engineering, 43(1–2), 99–111. https://doi.org/10.1016/j.petrol.2004.01.004

Shen, X., Zhao, L., Ding, Y., Liu, B., Zeng, H., Zhong, L., & Li, X. (2011). Foam, a promising vehicle to deliver nanoparticles for vadose zone remediation. Journal of Hazardous Materials, 186(2–3), 1773–1780. https://doi.org/10.1016/j.jhazmat.2010.12.071

Szafranski, R., Lawson, J. B., Hirasaki, G. J., Miller, C. A., Akiya, N., King, S., Jackson, R. E., Meinardus, H., & Londergan, J. (1998). Surfactant/foam process for improved efficiency of aquifer remediation. Structure, Dynamics and Properties of Disperse Colloidal Systems, 162–167. https://doi.org/10.1007/bfb0118126

Turta, A., & Singhal, A. (2002). Field Foam Applications in Enhanced Oil Recovery Projects: Screening and Design Aspects. Journal of Canadian Petroleum Technology, 41(10). https://doi.org/10.2118/02-10-14

Um, J. Y., Lee, G., Song, S. H., Hong, S., & Lee, M. (2013). Pilot Scale Feasibility Test of In-situ Soil Flushing by using "Tween 80" Solution at Low Concentration for the Xylene Contaminated Site. Journal of Soil and Groundwater Environment, 18(6), 38–47. https://doi.org/10.7857/jsge.2013.18.6.038

Wang, S., & Mulligan, C. N. (2004). An evaluation of surfactant foam technology in remediation of contaminated soil. Chemosphere, 57(9), 1079–1089. https://doi.org/10.1016/j.chemosphere.2004.08.019

Yuniati, M. D. (2018). Bioremediation of petroleum-contaminated soil: A Review. IOP Conference Series: Earth and Environmental Science, 118, 012063. https://doi.org/10.1088/1755-1315/118/1/012063

Namdar-Zanganeh, M., Kam, S.I., La Force T., and Rossen, W.R. (2011). The Method of Characteristics Applied to Oil Displacement by Foam. SPE Journal, 16(1), 8-23.

Zhang, T., Lowry, G. V., Capiro, N. L., Chen, J., Chen, W., Chen, Y., Dionysiou, D. D., Elliott, D. W., Ghoshal, S., Hofmann, T., Hsu-Kim, H., Hughes, J., Jiang, C., Jiang, G., Jing, C., Kavanaugh, M., Li, Q., Liu, S., Ma, J., . . . Alvarez, P. J. J. (2019). In situ remediation of subsurface contamination: opportunities and challenges for nanotechnology and advanced materials. Environmental Science: Nano, 6(5), 1283–1302. https://doi.org/10.1039/c9en00143c

Zhong, L., Mayer, A. S., & Pope, G. A. (2003). The effects of surfactant formulation on nonequilibrium NAPL solubilization. Journal of Contaminant Hydrology, 60(1–2), 55–75. https://doi.org/10.1016/s0169-7722(02)00063-3

Vita

Betty Lucy Cepeda-Salgado, born in Quito, Ecuador, worked as a field engineer in oil service companies in the Amazon rainforest after receiving her bachelor's degree from Escuela Superior Politecnica del Litoral. She has held volunteering positions in the Society of Petroleum Engineers at a local, regional, and international level. After spending time in the field, she decided to move on to enter the Craft and Hawkins Department of Petroleum Engineering at Louisiana State University after obtaining a scholarship from the Fulbright Commission and her home country. Upon completion of her master's degree in May 2023, she will begin to work on her doctorate.